Effective radius and droplet spectral width from in-situ aircraft observations in trade-wind cumuli during RICO

S. Arabas,[1] H. Pawlowska,[1] and W. W. Grabowski[2]

[1] This paper presents statistics of cloud microphysical properties of shallow tropical cumuli observed by a research aircraft during RICO field campaign. Cloud properties are derived from 10 Hz (about 10 m spatial distance) Fast-FSSP data in four different flights. The motivation comes from similar analyses of either aircraft data from stratocumulus clouds or remote-sensing data of tropical cumuli. In the lowest few hundred meters, the standard deviation of the droplet size distribution σ_r and the relative dispersion, the ratio of σ_r and the mean radius, are similar to stratocumulus clouds, but they are significantly larger in the upper half of the cloud field depth. The frequency distribution of the effective radius is significantly narrower than in the remote-sensing observations in the middle and upper third of the cloud field. These results can be used in parameterizations and validations of cloud microphysics in numerical models of various complexity. **Citation:** Arabas, S., H. Pawlowska, and W. W. Grabowski (2009), Effective radius and droplet spectral width from in-situ aircraft observations in trade-wind cumuli during RICO, *Geophys. Res. Lett.*, *36*, L11803, doi:10.1029/2009GL038257.

1. Introduction

[2] Representation of clouds and cloud-related small-scale processes remains the largest challenge in modeling climate and climate change. Shallow boundary layer clouds, such as subtropical stratocumulus and trade-wind cumulus, are especially important for the Earth climate because of their contrasting effects on solar (shortwave) and Earth thermal (longwave) radiation. Boundary layer clouds reflect back to space a significant fraction of incoming solar radiation, but—in contrast to deep tropical convection—their impact on the top-of-the-atmosphere outgoing long-wave radiation is relatively small. Boundary layer clouds have been shown to play the key role in the climate change and climate sensitivity [e.g., *Bony and Dufresne*, 2005]. For the cloud albedo, microphysical properties of these clouds (the concentration and mean size of cloud droplets, the width of cloud droplet spectrum, and their spatial variability) are of particular importance. Recent modeling studies [e.g., *Chosson et al.*, 2004, 2007; *Grabowski*, 2006; *Slawinska et al.*, 2008] show that assumptions concerning microphysical evolution of boundary layer clouds (the homogeneity of cloud-environment mixing in particular) significantly affect the mean albedo of the cloud field. Cloud observations provide a reference to which results from numerical modeling can be compared, and they can guide developments and/or improvements of the model microphysical schemes. This paper presents selected cloud microphysical parameters observed by an instrumented aircraft during the RICO (Rain In Cumulus over the Ocean) field experiment [see *Rauber et al.*, 2007].

[3] Motivation for the current analysis comes from two previously published studies. First, *Pawlowska et al.* [2006] discussed *in-situ* aircraft observations in eight cases of marine stratocumulus investigated during the Second Aerosol Characterization Experiment (ACE-2) in the eastern subtropical Atlantic. For a given flight (i.e., for given characteristics of the cloud condensation nuclei, CCN), local droplet concentration varied considerably, but the standard deviation of the cloud droplet spectrum was typically in the range of 1 to 2 μm. Moreover, the width did not vary systematically between pristine and polluted clouds, and it showed a surprisingly small difference between near-adiabatic and diluted cloud regions. The current study investigates whether the conclusions drawn from stratocumulus observations are equally applicable to shallow cumulus clouds. Second, *McFarlane and Grabowski* [2007] presented results from ground-based remote sensing of optical properties of tropical shallow convective clouds over the Nauru Atmospheric Radiation Measurement (ARM) site. The analysis focused on the effective radius of cloud droplets, the ratio between the third and the second moment of the cloud droplets size distribution. The effective radius is typically slightly larger than the mean volume radius [e.g., *Martin et al.*, 1994; *Pawlowska and Brenguier*, 2000] and the ratio between the two depends on the width of the droplet spectrum. Remote sensing data suggest that, at a given height, the effective radius shows large spatial variability, with its histogram relatively narrow near the cloud base, and widening and becoming bimodal at higher elevations [see *McFarlane and Grabowski*, 2007, Figure 2]. In the upper half of the cloud field, the peak at large values corresponds to droplets with radii several micrometers smaller than the adiabatic values, and the peak at small values corresponds to droplet sizes similar to those near the cloud base. Availability of *in-situ* aircraft observations collected during RICO allows comparing remote sensing and *in-situ* data.

[4] The next section provides a brief overview of the RICO data used in the analysis. Selected results are presented in section 3, and their brief summary and discussion in section 4 concludes the paper.

2. Aircraft Observations During RICO

[5] RICO field project [*Rauber et al.*, 2007] took place in the Antilles in December 2004 and January 2005. The

---

[1]Institute of Geophysics, University of Warsaw, Warsaw, Poland.
[2]National Center for Atmospheric Research, Boulder, Colorado, USA.

campaign included airborne, ground-based, and shipboard measurements. Current analysis is based on cloud micro-physical *in-situ* observations using NSF/NCAR C-130Q research aircraft. Cloud microphysical properties discussed here are derived mainly from measurements performed using the Fast-FSSP optical cloud droplet spectrometer [*Brenguier et al.*, 1998; *Burnet and Brenguier*, 2002]. The research flights carried out during RICO were composed of several constant-altitude legs and two vertical sounding legs at the beginning and at the end of each flight. Each of the 19 flights lasted about eight hours, of which about 5 to 10% were spent in clouds. Most of the analyzed data presented here were processed with 10 Hz frequency resulting in an about 10 m spatial resolution. In the case of the Fast-FSSP such time resolution represents sampling of approximately one cubic centimeter of air in each 10 Hz sample. The choice of the 10 Hz sampling rate (used previously by *Pawlowska et al.* [2006] and also by *Burnet and Brenguier* [2007]) represents a compromise between a ten times higher spatial resolution and an approximately threefold increase in uncertainty resulting from a lower number of counted particles when compared to 1 Hz sampling. The latter should be less significant when employing the flight-long statistics. Also, a better cloud-edge detection is obtained with the 10 Hz sampling rate.

[6] Droplet spectral parameters were derived from the 255-bin description of the 1 to 24 μm range of droplet radius spectrum measured by the Fast-FSSP. The key reason for choosing the Fast-FSSP for the present analysis is the high spectral resolution of the instrument. A comparison of the results obtained using other probes available on the aircraft (such as FSSP-100, PVM-100A, King probe) is discussed by *Arabas* [2008]. In general, we are confident that general features of cloud parameters presented here only weakly depend on the choice of the instruments. The sensitivity to the selected sampling rate (i.e., 10 Hz vs. 1 Hz) is noticeable for selected parameters, a good example being the adiabatic fraction (AF), whose statistics show an expected shift of the distribution toward larger values with higher sampling rate [cf. *Gerber et al.*, 2008, Figure 1].

[7] Overall, seven flight-long Fast-FSSP datasets were available and analyzed. Here, we present results of flight-long statistics for four diverse flights. Three of the selected flights (rf06, rf09, and rf12; the latter the same as of *Gerber et al.* [2008]) represent examples of observed cloud fields with increasing depths, the smallest for the rf06 (about 600 m) and the largest for the rf12 (about 1,200 m). The fourth flight (rf07) is selected because it features clouds at two different altitude ranges. The choice of flight-long statistics is dictated by the need for a comparison of the RICO *in-situ* measurements with long-term remote-sensing retrievals [e.g., *McFarlane and Grabowski*, 2007] as well as domain-averaged cloud model results [e.g., *Slawinska et al.*, 2008]. Such an approach enables one to assess typical properties of an ensemble of clouds of similar origin and preserves day-to-day variability of the cloud field (e.g., the cloud depth), but it averages any differences in cloud microphysics related to a particular stage of the cloud evolution.

[8] All results are analysed as a function of height above the cloud base, with the cloud base height assumed constant throughout the flight. The cloud base heights were chosen with a 50 m resolution with the aid of liquid water content profile analysis and were set to 500 m (for rf07 and rf09) or 550 m (for rf06 and rf12) above sea level. These appear consistent with the thermodynamic profiles in the sub-cloud layer (not shown). The considered range of altitudes above cloud base (1500 m) was divided into 100 m deep classes (or bins). Histograms representing frequency distributions of selected parameters were constructed for each altitude class separately and then presented on diagrams showing the frequency distributions as a function of height. Altitude classes representing marginal statistical significance (small number of data points) were discarded.

[9] The analysis considers all in-cloud data points for selected flights. An in-cloud data point is defined using the droplet concentration threshold ($N > 20\ cm^{-3}$) applied to the Fast-FSSP data (a condition representing both a cloud-edge threshold and a criterion of statistical significance for calculation of the droplet spectral parameters). In addition, analysis considers only in-cloud data points void of drizzle. A volume of air is considered to contain drizzle when the 2D-C optical array probe registered over 10 l^{-1} particles larger than 45 μm (the 2D-C 1 Hz data was linearly interpolated to 10 Hz sampling rate for this purpose). The 2D-C probe was chosen from other drizzle-sensitive probes for it was mounted on the same wing of the aircraft as the Fast-FSSP (e.g., 30 meters closer than the 260X probe). This resulted in neglecting 10 to 20% of in-cloud data points, and this fraction proved to be insensitive to the threshold value within the $2-20\ l^{-1}$ range. Such filtering addresses the issue of drop shattering on the Fast-FSSP arms. It also assures that the analysed data subset is limited to the areas in cloud where the actual droplet spectrum did not overlap the Fast-FSSP spectral range.

[10] In both cases where the cloud-field depth reached over 1000 m (i.e., rf07 and rf12) precipitation was observed beneath the cloud-base. According to mission scientist reports (http://catalog.eol.ucar.edu/rico/), no rain shafts were observed in the other two cases of less developed cumuli (rf06 and rf09). The cloud-field depth is also correlated with the amount of drizzle drops sensed by the 2DC probe because the fraction of records discarded due to the drizzle threshold was higher for the rf07 and rf12 cases.

3. Results

[11] Figure 1 summarizes results for the droplet concentration N and selected droplet spectral parameters: the mean radius $\bar{r}$, its standard deviation σ_r, and relative dispersion $d = \sigma_r/\bar{r}$ for the four selected flights. Histogram bins at each height have constant width selected as 5 cm^{-3} for N, 0.5 μm for $\bar{r}$, 0.2 μm for σ_r, and 0.025 for d and are represented in the diagrams by pixel-like shaded rectangles, with the vertical extent representing the 100-m altitude bin. Histograms representing frequency distributions of selected parameters are constructed for each altitude class separately and then presented on diagrams as a function of height. At each height, the histograms are presented using a color scale defined as follows [e.g., see *Einmahl and Mason*, 1992]. The darkest shade marks the most frequently occurring bins, such that the sum of their frequency of occurrence equals 20%. The darkest plus the subsequent lighter shade mark the most frequently occurring bins such that the sum of their
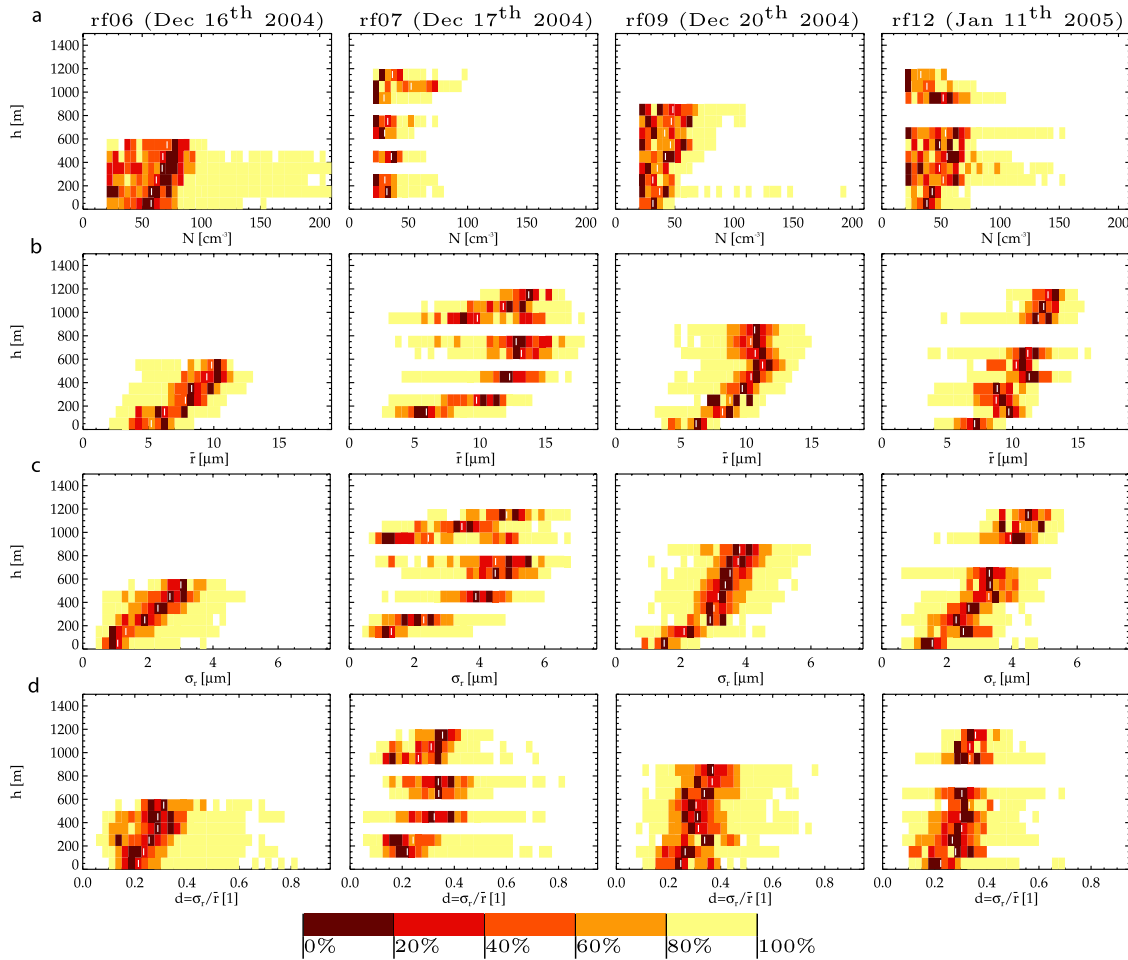
Figure 1. Statistics of droplet-spectrum and concentration measurements from RICO flights rf06, rf07, rf09, and rf12 as a function of height. (a) Droplet concentration N, (b) the mean radius $\bar{r}$, (c) the standard deviation of radius σ_r, and (d) the relative dispersion $d = \sigma_r/\bar{r}$. See text for details.

frequency of occurrence equals 40%. This procedure is repeated until 100% is reached, that is, all measured values are included in the diagram. Such diagrams differ from the contoured frequency by altitude diagrams (CFADs, as used, e.g., by *McFarlane and Grabowski* [2007]) because the shade-frequency relationship is constructed for each level separately. In particular, for a CFAD, a wide histogram with relatively low frequencies over wide range of bins is represented with a subset of shades thus hiding details (e.g., multi-modality) of the histogram. In our procedure, all shades are utilized at each height separately. In addition, Figure 1 also shows median values of the distributions using white vertical bars.

[12] In all four flights, 80% of samples were characterized by droplet concentrations lower than $100 \ cm^{-3}$ (and even lower than $50 \ cm^{-3}$ for the rf07 and rf09). The high-concentration tail (related to about 10% of the least frequent values) observed during the rf06 flight comes from a few clouds with high concentration (up to $350 \ cm^{-3}$) of small droplets (in the 2 to $5 \ \mu m$ radius range). This feature is also present in the data obtained by the FSSP-100, and is attributed to the fact that the aircraft repeatedly crossed a large-scale plume of more polluted air, evidently rich in aerosol particles acting as CCN (see *Hudson and Mishra*

[2007] for discussion of CCN measurements beneath the cloud-base during these RICO flights). Otherwise, the observed low droplet concentrations indicate that clouds formed in the pristine maritime air.

[13] The mean radius statistics presented in Figure 1 show an increase of droplet size until approximately half of the depth of the cloud field. Above, the increase of $\bar{r}$ is less pronounced. The histograms are quite wide, implying a significant spatial variability of $\bar{r}$, most likely related to entrainment and mixing processes. The standard deviation of the droplet spectra σ_r (Figure 1c) shows its gradual increase with height, from values in the 1 to $2 \ \mu m$ in the lowest couple hundred meters, to values as large as $5 \ \mu m$ near the cloud top. The values in the lowest $100–200 \ m$ of the cloud field are similar to those observed in stratocumulus in ACE-2 [see *Pawlowska et al.*, 2006, Figure 2]. The strongest resemblance is observed for the lowest adiabatic fraction cases from the ACE-2 data analysis. Large values of σ_r, in the middle and upper parts of the cloud field, are again most likely related to entrainment and mixing, and seem consistent with results presented in particular by *Burnet and Brenguier* [2007, Figure 9]. The relative dispersion d (Figure 1d) is about 0.2 in the lowest couple hundred meters (again consistent with the data from pristine
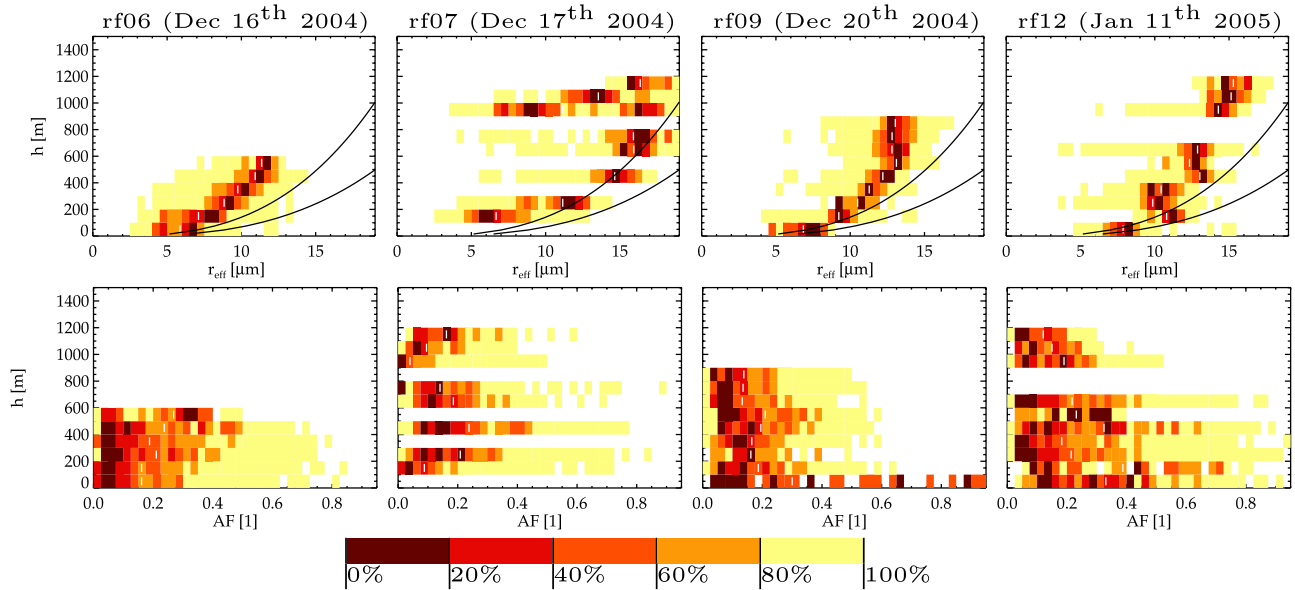
Figure 2. Same as Figure 1, but for the effective radius r_{eff} and adiabatic fraction AF values. Effective radius for adiabatic clouds with droplet concentrations of 50 and 100 cm^{-3} are shown by solid lines (larger r_{eff} values correspond to the concentration of 50 cm^{-3}).

cases in ACE-2 [*Pawlowska et al.*, 2006, Figure 2]). It increases slightly at higher levels, with typical values between 0.2 and 0.4. However, the range of values of d observed during RICO is relatively wide (from 0.1 to 0.8), while the spread of d reported for ACE-2 was significantly smaller [cf. *Pawlowska et al.*, 2006, Figures 2 and 3].

[14] A closer analysis of the rf07 data suggests that the aircraft probed two separate layers of clouds. On that day, the lower cloud layer was capped by a shallow layer of stratiform clouds (described in the report of the flight crew and visible on the images from the aircraft-cockpit camera). This seems to explain structures suggesting a second cloud base around 900 m in the plots of $\bar{r}$ and σ_r in Figure 1. Such multi-layer situation might be an example of a difficult case for the retrieval procedure applied to the remote-sensing data presented by *McFarlane and Grabowski* [2007] where a wide bimodal shape of effective radius frequency distribution was reported at higher parts of the clouds.

[15] Figure 2 presents results of the analysis of the effective radius r_{eff} (Figure 2, top) and the adiabatic fraction AF (Figure 2, bottom) in the format similar to Figure 1 (with histogram bin widths of 0.5 μm for r_{eff} and 0.025 for AF) and for the same four flights. As by *McFarlane and Grabowski* [2007], an adiabatic parcel model was used to obtain the adiabatic liquid water content above the cloud base (assumed to be constant throughout the flight). The ratio between the observed water content (obtained from the Fast-FSSP measurements) and the adiabatic limit, the adiabatic fraction AF, describes the local dilution of a probed cloud volume. Figure 2 should be compared to *McFarlane and Grabowski* [2007, Figures 1 and 2] (bearing in mind the six-month long period of measurements represented by the remote sensing statistics). In agreement with many previous observations, RICO clouds are significantly diluted by entrainment [see, e.g., *Gerber et al.*, 2008]. However, the dilution is not as strong as that of *McFarlane and Grabowski* [2007]. One needs to keep in mind, however, that the values

of AF depend on the choice of the cloud-base altitude. Since the analysis presented here assumes a constant cloud-base height, the AF values are characterized by additional uncertainties, especially near the cloud base.

[16] The most striking is the difference in the statistics of the effective radius obtained in the current study and those presented by *McFarlane and Grabowski* [2007]. In particular, the distributions here are monomodal (except for the flight rf07 which featured two separate cloud layers as discussed above), with the maximum frequency of values roughly corresponding to the larger r_{eff} values of *McFarlane and Grabowski* [2007, Figure 2].

4. Summary

[17] This paper presents results of aircraft data analysis from four selected flights in RICO. The goal is to obtain relationships that are needed in cloud model microphysical parameterizations, for instance, in the two-moment bulk microphysics scheme of *Morrison and Grabowski* [2007, 2008] where the width of the cloud droplet spectrum has to be prescribed. In addition, the width of the spectrum has been shown to affect the relationship between the effective radius and the mean volume radius [*Martin et al.*, 1994; *Liu and Daum*, 2000]. The values of the relative dispersion observed in RICO cumuli are larger than those in ACE-2 and in previous stratocumulus observations [e.g., *Martin et al.*, 1994].

[18] As for the frequency distribution of the effective radius, there are significant differences between results presented here and those of *McFarlane and Grabowski* [2007, Figure 2]. In particular, the aircraft data show much narrower distributions, approximately corresponding to the peak at larger droplet sizes of *McFarlane and Grabowski* [2007, Figure 2]; that is, those a few micrometers smaller than the adiabatic size. The bimodality of the effective radius frequency distribution is not observed in the in-situ

data except for the flight rf07 where the aircraft probed two different layers of clouds. We hope that additional analyses of the aircraft and remote-sensing data currently underway will help to understand these significant differences.

References

Arabas, S. (2008), Microphysical properties of shallow convective clouds—The RICO case study (in Polish), M.S. thesis, Fac. of Phys., Univ. of Warsaw, Warsaw, Poland.

Bony, S., and J.-L. Dufresne (2005), Marine boundary layer clouds at the heart of tropical cloud feedback uncertainties in climate models, *Geophys. Res. Lett.*, *32*, L20806, doi:10.1029/2005GL023851.

Brenguier, J.-L., T. Bourrianne, A. Coelho, J. Isbert, R. Peytavi, D. Trevarin, and P. Weschler (1998), Improvements of droplet size distribution measurements with the Fast-FSSP (forward scattering spectrometer probe), *J. Atmos. Oceanic Technol.*, *15*, 1077–1090.

Burnet, F., and J.-L. Brenguier (2002), Comparison between standard and modified Forward Scattering Spectrometer Probes during the Small Cumulus Microphysics Study, *J. Atmos. Oceanic Technol.*, *19*, 1516–1531.

Burnet, F., and J.-L. Brenguier (2007), Observational study of the entrainment-mixing process in warm convective clouds, *J. Atmos. Sci.*, *64*, 1995–2011.

Chosson, F., J.-L. Brenguier, and M. Schröder (2004), Radiative impact of mixing processes in boundary layer clouds, in *Proceedings of the 14th International Conference on Clouds and Precipitation*, pp. 371–374, Int. Assoc. of Meteorol. and Atmos. Sci., Bologna, Italy.

Chosson, F., J.-L. Brenguier, and L. Schüller (2007), Entrainment-mixing and radiative transfer simulation in boundary-layer clouds, *J. Atmos. Sci.*, *54*, 2670–2682.

Einmahl, J., and D. Mason (1992), Generalized quantile processes, *Ann. Stat.*, *20*, 1062–1078.

Gerber, H., G. Frick, J. Jensen, and J. Hudson (2008), Entrainment, mixing, and microphysics in trade-wind cumulus, *J. Meteorol. Soc. Jpn.*, *86*, 87–106.

Grabowski, W. W. (2006), Indirect impact of atmospheric aerosols in idealized simulations of convective-radiative quasi-equilibrium, *J. Clim.*, *19*, 4664–4682.

Hudson, J. G., and S. Mishra (2007), Relationships between CCN and cloud microphysics variations in clean maritime air, *Geophys. Res. Lett.*, *34*, L16804, doi:10.1029/2007GL030044.

Liu, Y., and P. H. Daum (2000), Spectral dispersion of cloud droplet size distributions and the parametrization of cloud droplet effective radius, *Geophys. Res. Lett.*, *27*, 1903–1906.

Martin, G. M., D. W. Johnson, and A. Spice (1994), The measurement and parameterization of effective radius of droplets in warm stratocumulus clouds, *J. Atmos. Sci.*, *51*, 1823–1842.

McFarlane, S. A., and W. W. Grabowski (2007), Optical properties of shallow tropical cumuli derived from ARM ground-based remote sensing, *Geophys. Res. Lett.*, *34*, L06808, doi:10.1029/2006GL028767.

Morrison, H., and W. W. Grabowski (2007), Comparison of bulk and bin warm rain microphysics models using a kinematic framework, *J. Atmos. Sci.*, *64*, 2839–2861.

Morrison, H., and W. W. Grabowski (2008), Modeling supersaturation and subgrid-scale mixing with two-moment bulk warm microphysics, *J. Atmos. Sci.*, *65*, 792–812.

Pawlowska, H., and J.-L. Brenguier (2000), Microphysical properties of stratocumulus clouds during ACE-2, *Tellus, Ser. B*, *52*, 868–887.

Pawlowska, H., W. W. Grabowski, and J.-L. Brenguier (2006), Observations of the width of cloud droplet spectra in stratocumulus, *Geophys. Res. Lett.*, *33*, L19810, doi:10.1029/2006GL026841.

Rauber, R., et al. (2007), Rain in shallow cumulus over the ocean—The RICO campaign, *Bull. Am. Meteorol. Soc.*, *88*, 1912–1928.

Slawinska, J., W. W. Grabowski, H. Pawlowska, and A. A. Wyszogrodzki (2008), Optical properties of shallow convective clouds diagnosed from a bulk-microphysics large-eddy simulation, *J. Clim.*, *21*, 1639–1647.

―――――――――――――

S. Arabas and H. Pawlowska, Institute of Geophysics, University of Warsaw, Pasteura 7, 02-093 Warsaw, Poland. (sarabas@igf.fuw.edu.pl; hanna.pawlowska@igf.fuw.edu.pl)

W. W. Grabowski, National Center for Atmospheric Research, P.O. Box 3000, Boulder, CO 80307-3000, USA. (grabow@ucar.edu)